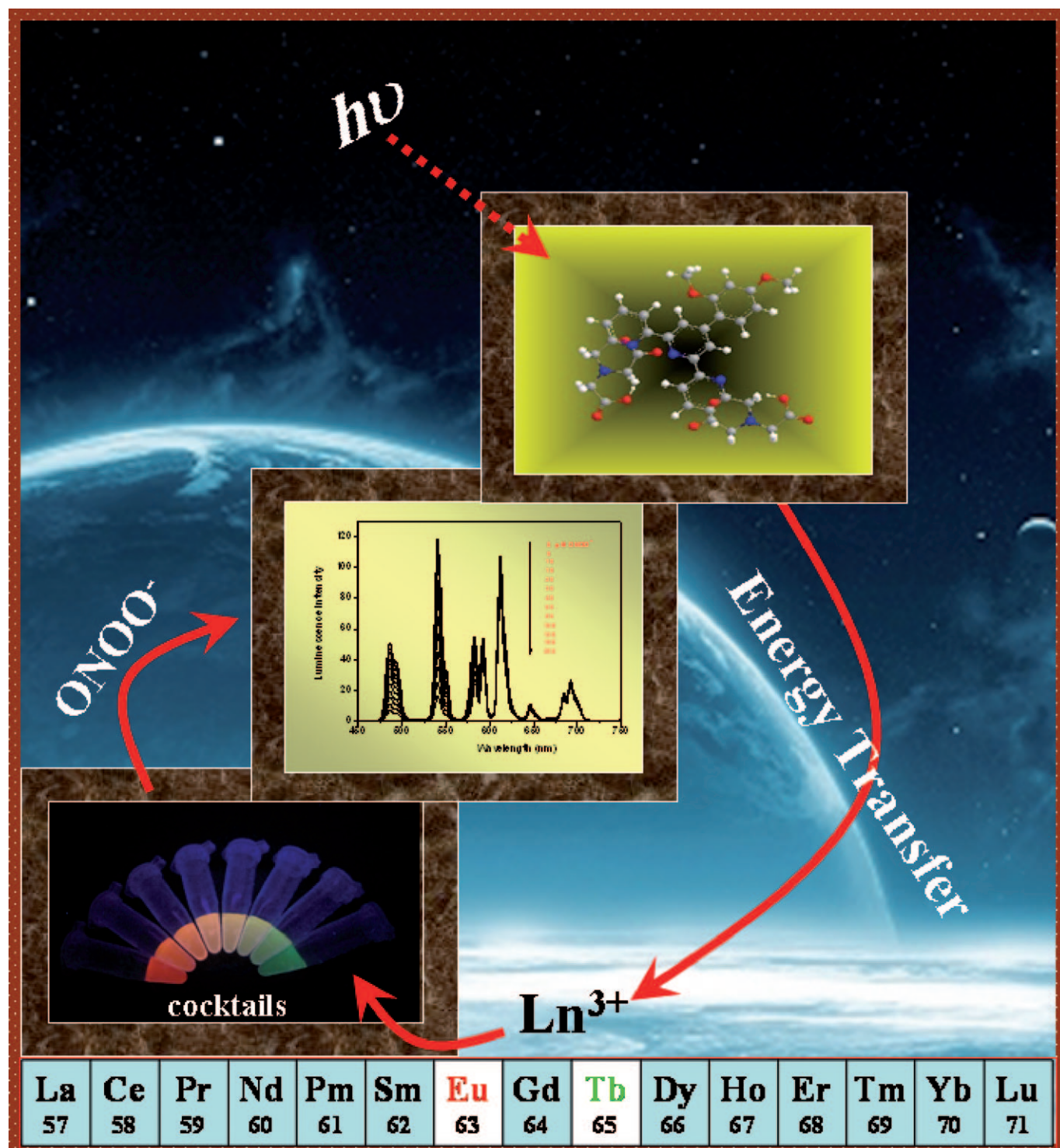


A Lanthanide-Complex-Based Ratiometric Luminescent Probe Specific for Peroxynitrite

Cuihong Song,^[a] Zhiqiang Ye,^[b] Guilan Wang,^[b] Jingli Yuan,^{*,[a, b]} and Yafeng Guan^{*,[a]}



Abstract: A lanthanide-complex-based ratiometric luminescence probe specific for peroxynitrite (ONOO^-), 4'-(2,4-dimethoxyphenyl)-2,2':6',2''-terpyridine-6,6''-diyl]bis(methylenenitrilo)tetrakis-(acetate)- $\text{Eu}^{3+}/\text{Tb}^{3+}$ ($[\text{Eu}^{3+}/\text{Tb}^{3+}(\text{DTTA})]$), has been designed and synthesized. Both $[\text{Eu}^{3+}(\text{DTTA})]$ and $[\text{Tb}^{3+}(\text{DTTA})]$ are highly water soluble with large stability constants at $\approx 10^{20}$, and strongly luminescent with luminescence quantum yields of 10.0 and 9.9%, respectively, and long lumines-

cence lifetimes of 1.38 and 0.26 ms, respectively. It was found that the luminescence of $[\text{Tb}^{3+}(\text{DTTA})]$ could be quenched by ONOO^- rapidly and specifically in aqueous buffers, while that of $[\text{Eu}^{3+}(\text{DTTA})]$ did not respond to the addition of ONOO^- . Thus, by simply mixing $[\text{Eu}^{3+}(\text{DTTA})]$ and

$[\text{Tb}^{3+}(\text{DTTA})]$ in an aqueous buffer, a ratiometric luminescence probe specific for time-gated luminescence detection of ONOO^- was obtained. The performance of $[\text{Tb}^{3+}(\text{DTTA})]$ and $[\text{Eu}^{3+}/\text{Tb}^{3+}(\text{DTTA})]$ as the probes for luminescence imaging detection of ONOO^- in living cells was investigated. The results demonstrated the efficacy and advantages of the new ratiometric luminescence probe for highly sensitive luminescence bioimaging application.

Keywords: analytical methods • cell imaging • lanthanides • luminescence • peroxynitrite

Introduction

Peroxyntirite (ONOO^-), a short-lived reactive oxygen species (ROS), has attracted much attention, because it can cause serious damage to living systems.^[1] It is generated in biological systems through the spontaneous coupling reaction of nitric oxide (NO) and superoxide radical ($\text{O}_2^{\cdot-}$). This peroxide in itself is very reactive; however, its biological action is particularly notorious under elevated cell/tissue rates of NO and/or $\text{O}_2^{\cdot-}$ production. Increasing evidence has shown that aberrant ONOO^- activities may contribute to a series of human diseases including inflammatory processes, ischemic reperfusion injury, multiple sclerosis, stroke, cancer, and neurodegenerative disorders.^[2]

Until now, several approaches have been developed for the detection of ONOO^- , including UV/Vis spectroscopy, chemiluminescence, amperometry and electron spin resonance, and immunohistochemistry.^[3] Due to the short lifetime, low concentration, high activity, and elusive nature of ONOO^- in vivo, the precise pathogenic role of ONOO^- in biological systems is still not very clear. To study the physiological role of ONOO^- in living cells or tissues, a fluorescent probe technique was developed as a useful tool, because of its high sensitivity, selectivity, and experimental convenience.^[4] Though a number of fluorescent probes^[5] have been developed and are widely used to monitor ONOO^- in various biological systems, for example, dihydrorhodamine-123

(DHR-123), dihydrodichlorofluorescein (DCFH), and so forth, the specificity of these probes is low and the exact mechanism of the oxidation of these probes by ONOO^- is still a question of debate. Thus, there is an imperative need to develop new ONOO^- -specific fluorescent probes. In this regard, several such probes have been synthesized recently by using mechanism-based molecular design, involving either aromatic nitration (NiSPYs)^[6] or ketone oxidation reactions (HKGreen).^[7] These probes are based on a photoinduced electron transfer (PET) mechanism and show dramatic fluorescence enhancement upon reaction with ONOO^- . They suffer, however, from a few limitations: poor water solubility and photostability, small Stokes shift, and inferior intracellular retentions. Furthermore, all the reported ONOO^- fluorescent probes only show changes in fluorescent intensity, which could be influenced by many factors, for example, excitation intensity, dye concentration, sample environment, and so forth. Thus, a ratiometric fluorescent probe that can eliminate most or all ambiguities by self-calibration of two emission bands^[8] for ONOO^- is highly desirable.

It has long been appreciated that lanthanide complexes afford considerable scope for the development of novel chemical entities that can be used as luminescence probes, as components of optoelectronic devices, or as key sensor materials.^[9] Luminescent lanthanide complexes have long luminescence lifetimes, large Stokes shifts, and sharp emission profiles; these properties enable them to be used for microsecond time-gated (or time-resolved) luminescence measurements to eliminate fast decaying autofluorescence from biological specimens, scattering lights, and optical components. Recently, we have demonstrated that lanthanide complexes are useful time-gated luminescence probes for ROS. Three lanthanide complex-based luminescent probes have been successfully developed for the highly sensitive and selective time-gated luminescence detection of singlet oxygen ($^1\text{O}_2$).^[9a,10] Based on the above, we have attempted to develop the lanthanide complex-based ratiometric luminescence probe for specific detection of ONOO^- , since three recent reports have demonstrated that the bis-lanthanide ensemble

[a] C. Song, Prof. J. Yuan, Prof. Y. Guan
Department of Instrumentation and Analytical Chemistry
Dalian Institute of Chemical Physics
Chinese Academy of Sciences, Dalian 116023 (China)
Fax: (+86)411-84706293
Fax: (+86)411-84379590
E-mail: jingliyuan@yahoo.com.cn
guanyafeng@dicp.ac.cn

[b] Dr. Z. Ye, Prof. G. Wang, Prof. J. Yuan
School of Chemistry, Dalian University of Technology
Dalian 116012 (China)

Supporting information for this article is available on the WWW under <http://dx.doi.org/10.1002/chem.201000528>.

consisting of a mixture of $\text{Eu}^{3+}/\text{Tb}^{3+}$ complexes can be used to generate ratiometric luminescence probes.^[11a-c]

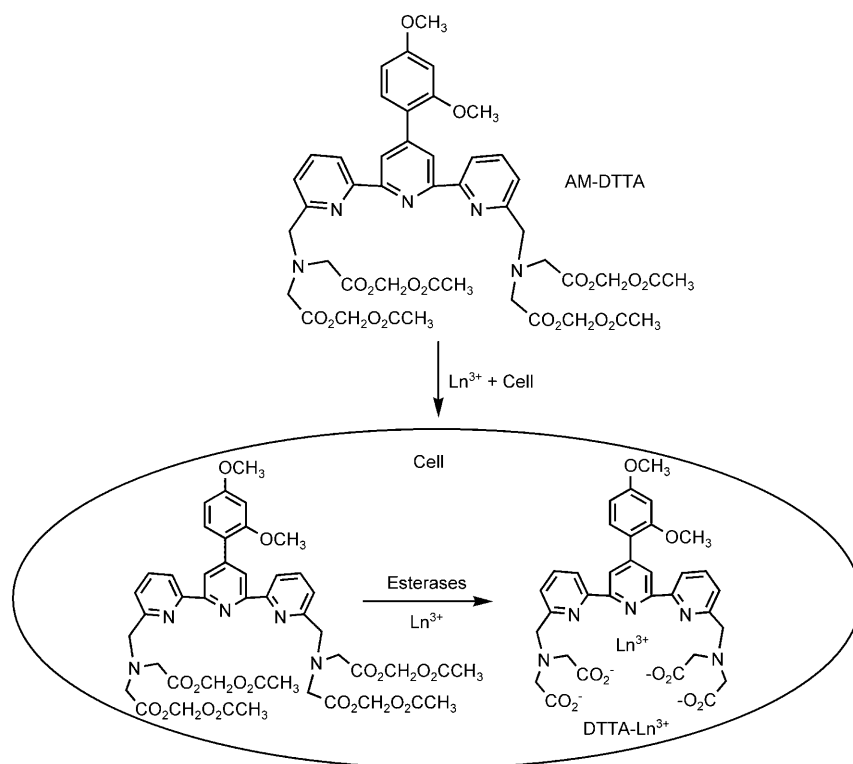
In this work, a new nonadentate ligand, [4'-(2,4-dimethoxyphenyl)-2,2':6',2''-terpyridine-6,6''-diyl]bis(methylenetri-*l*o)tetrakis(acetic acid) (DTTA, Scheme 1), was designed and synthesized. Both $[\text{Eu}^{3+}(\text{DTTA})]$ and $[\text{Tb}^{3+}(\text{DTTA})]$ complexes in aqueous buffers are highly luminescent with the same excitation pattern. After addition of ONOO^- , the luminescence of $[\text{Tb}^{3+}(\text{DTTA})]$ was dramatically decreased, whereas that of $[\text{Eu}^{3+}(\text{DTTA})]$ did not change. When the "cocktail" of $[\text{Eu}^{3+}/\text{Tb}^{3+}(\text{DTTA})]$ was used for the time-gated luminescence detection of ONOO^- , a bi-exponential correlation between the emission intensity ratio ($\text{Eu}^{3+}/\text{Tb}^{3+}$) and the ONOO^- concentration was obtained. To investigate the potential use of $[\text{Tb}^{3+}(\text{DTTA})]$ and the $[\text{Eu}^{3+}/\text{Tb}^{3+}(\text{DTTA})]$ mixture for the detection of ONOO^- in living cells, the cell permeable form of DTTA, acetoxymethyl ester of DTTA (AM-DTTA, Scheme 1), was also synthesized. Both AM-DTTA and Ln^{3+} (Eu^{3+} and Tb^{3+}) could be easily transferred into the cultured cells with ordinary incubation methods, and in the cells, accompanied by the rapid hydrolysis of AM-DTTA catalyzed by ubiquitous intracellular esterases,^[12a] the stable $[\text{Ln}^{3+}(\text{DTTA})]$ complex was formed (Scheme 1). This process is similar to the cell loading process of the Ca^{2+} luminescent probe Fura 2.^[12b] The $[\text{Tb}^{3+}(\text{DTTA})]$ - and $[\text{Eu}^{3+}/\text{Tb}^{3+}(\text{DTTA})]$ -loaded cells were used for the luminescence imaging detection of ONOO^- . The results suggest that the $\text{Eu}^{3+}/\text{Tb}^{3+}$ -complex-based ratiometric luminescence probe developed in this work could be

a very useful tool for long-term visualization and detection of ONOO^- in intact cells to elucidate the precise role of ONOO^- in various biological processes.

Results and Discussion

Probe design and characterization: The use of fluorescent probes is one of the most promising methods to analyze and clarify the roles of ROS in biological processes. Recent efforts in our laboratory have focused on the rational design of functional lanthanide luminescent probes for ROS. Compared with conventional organic probes, these lanthanide probes possess a unique advantage in that the luminescence measurement can be carried out with a time-gated mode to minimize the effect of background noise.^[13] Until now, although some organic-dye-based fluorescent probes for ONOO^- have been developed, a lanthanide-complex-based probe for ONOO^- , to our knowledge, has never been reported. In this work, a new lanthanide chelator—DTTA—was designed and synthesized by incorporating a 2,4-dimethoxyphenyl group into a (2,2':6',2''-terpyridine-6,6''-diyl)-bis(methylenetri-*l*o)tetrakis(acetic acid) moiety, since the former can specifically respond to ONOO^- ^[6] and the latter can form highly luminescent and stable complexes both with Eu^{3+} and Tb^{3+} ions in aqueous media.^[14]

The time-gated excitation and emission spectra of $[\text{Eu}^{3+}(\text{DTTA})]$ and $[\text{Tb}^{3+}(\text{DTTA})]$ are shown in Figure 1 (top). Both $[\text{Eu}^{3+}(\text{DTTA})]$ and $[\text{Tb}^{3+}(\text{DTTA})]$ show the excitation maximum wavelength at 335 nm with the same excitation pattern. The $[\text{Eu}^{3+}(\text{DTTA})]$ complex shows a typical Eu^{3+} emission pattern with a main emission peak at 612 nm (${}^5\text{D}_0 \rightarrow {}^7\text{F}_2$) and several side peaks centered at 584, 592, 646, and 692 nm; the $[\text{Tb}^{3+}(\text{DTTA})]$ complex shows a typical Tb^{3+} emission pattern with a main emission peak at 541 nm (${}^5\text{D}_4 \rightarrow {}^7\text{F}_5$) and several side peaks centered at 486, 581, and 617 nm. In an air-saturated 0.05 M borate buffer of pH 9.1, the luminescence quantum yield and lifetime of $[\text{Eu}^{3+}(\text{DTTA})]$ are 10.0% and 1.38 ms, respectively, and those of $[\text{Tb}^{3+}(\text{DTTA})]$ are 9.9% and 0.26 ms, respectively. The shorter luminescence lifetime of the Tb^{3+} complex is considered to be caused by the dissolved oxygen. In an argon-saturated buffer, the luminescence lifetime of the Tb^{3+} complex was measured to be



Scheme 1. Schematic diagram of the cell loading process of $[\text{Ln}^{3+}(\text{DTTA})]$ complex.

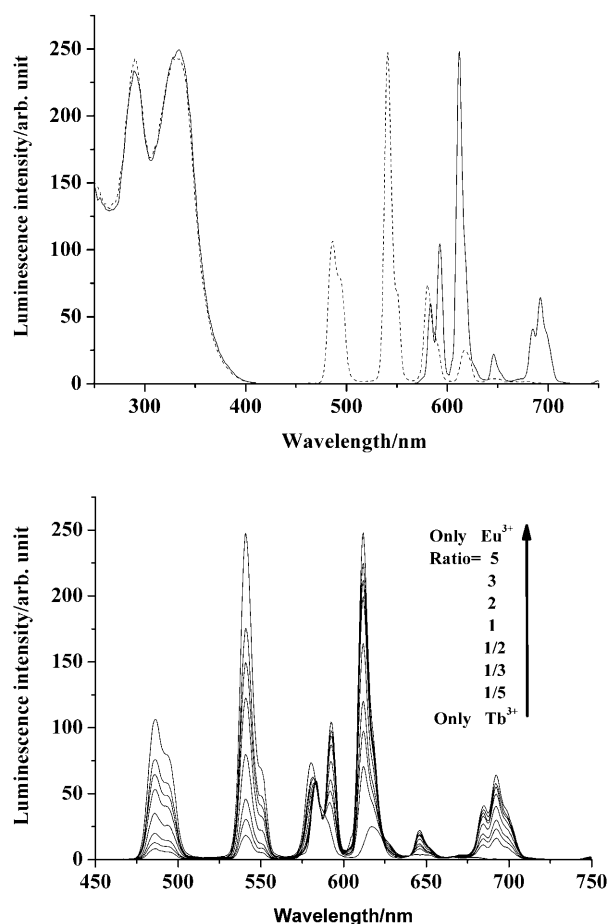


Figure 1. Top: Time-gated excitation and emission spectra of $[\text{Eu}^{3+}(\text{DTTA})]$ (2.0 μM , solid lines) and $[\text{Tb}^{3+}(\text{DTTA})]$ (2.0 μM , dash lines) in 0.05 M borate buffer of pH 9.1. Bottom: Time-gated emission spectra of $[\text{Eu}^{3+}/\text{Tb}^{3+}(\text{DTTA})]$ mixtures (total concentration of 2.0 μM) with different molar ratios of $\text{Eu}^{3+}/\text{Tb}^{3+}$ in 0.05 M borate buffer of pH 9.1.

0.68 ms, while that of the Eu^{3+} complex was almost unchanged (1.33 ms). Since DTTA can form highly luminescent complexes both with Eu^{3+} and Tb^{3+} ions, the $[\text{Eu}^{3+}/\text{Tb}^{3+}(\text{DTTA})]$ mixtures with different molar ratios of $\text{Eu}^{3+}/\text{Tb}^{3+}$ show different luminescence emission spectra when excited at the same wavelength (335 nm). Thus, by adjusting the relative amount of Eu^{3+} and Tb^{3+} , a variety of emission spectra were obtained (Figure 1, bottom). These results indicate that DTTA is an ideal $\text{Eu}^{3+}/\text{Tb}^{3+}$ chelator for a two-emission-wavelength signaling approach.

The $[\text{Eu}^{3+}(\text{DTTA})]$ and $[\text{Tb}^{3+}(\text{DTTA})]$ complexes show a high stability in aqueous media, because of the polyacid structure of the ligand. When $[\text{Eu}^{3+}(\text{DTTA})]$ and $[\text{Tb}^{3+}(\text{DTTA})]$ were exposed to fivefold excess of ethylenediamine tetraacetic acid, the conditional stability constants, measured by Verhoeven's method,^[15] were found to be 7.2×10^{20} and 1.6×10^{20} for $[\text{Eu}^{3+}(\text{DTTA})]$ and $[\text{Tb}^{3+}(\text{DTTA})]$, respectively. In addition, no significant changes in the luminescence intensities of the two complexes were observed after several weeks at room temperature. The average number (q) of coordinated water molecules in the first coor-

dination sphere of Eu^{3+} ion was 0.05, calculated by the equation $q = 1.2(1/\tau_{\text{H}_2\text{O}} - 1/\tau_{\text{D}_2\text{O}} - 0.25)^{[16]}$ ($\tau_{\text{D}_2\text{O}}$ and $\tau_{\text{H}_2\text{O}}$ are luminescence lifetimes of $[\text{Eu}^{3+}(\text{DTTA})]$ in D_2O and H_2O buffers, respectively). The effects of pH on the luminescence intensity and lifetime of $[\text{Ln}^{3+}(\text{DTTA})]$ (Ln^{3+} : Eu^{3+} or Tb^{3+}) were investigated by using 1.0 μM of $[\text{Ln}^{3+}(\text{DTTA})]$ in 0.05 M Tris-HCl buffers at different pHs ranging from 2 to 10 (Figure 2). The results show that both luminescence intensity and lifetime of $[\text{Ln}^{3+}(\text{DTTA})]$ are not remarkably affected (<5%) by the pH in the range of pH 3.0–10, indicating that the $[\text{Ln}^{3+}(\text{DTTA})]$ complex can be used as a luminescent probe in weakly acidic, neutral, and weakly basic buffers.

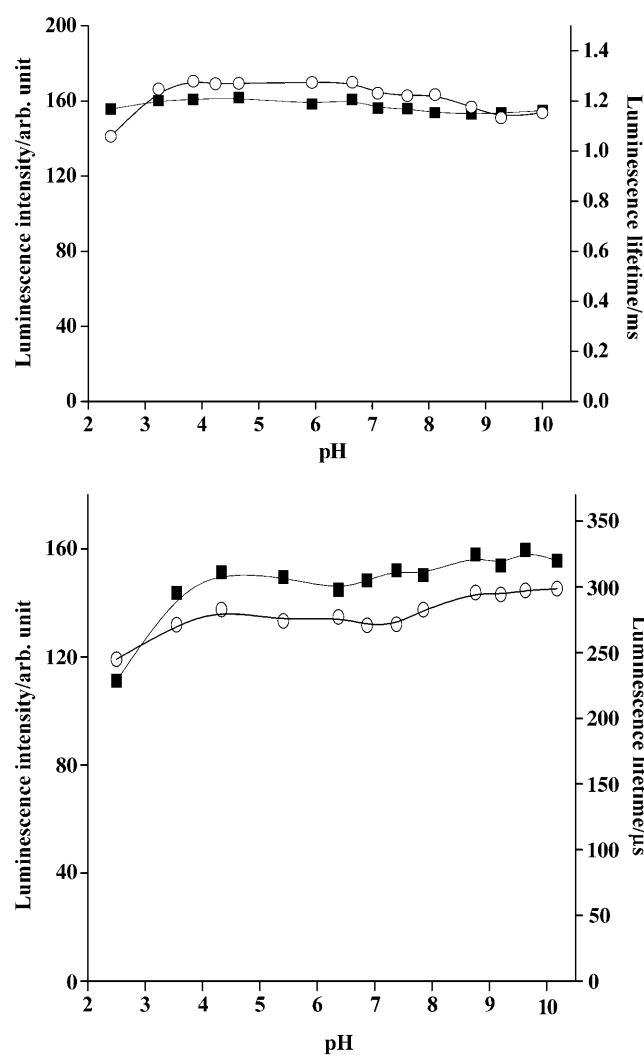


Figure 2. Effects of pH on the luminescence intensity (black square) and lifetime (circle) of $[\text{Eu}^{3+}(\text{DTTA})]$ (top) and $[\text{Tb}^{3+}(\text{DTTA})]$ (bottom).

Reaction between $[\text{Ln}^{3+}(\text{DTTA})]$ and ONOO^- : The effects of ONOO^- on the optical properties including luminescence intensity, lifetime, and time-gated luminescence intensity of the $[\text{Ln}^{3+}(\text{DTTA})]$ complexes were investigated. Figure 3 shows the optical responses of $[\text{Eu}^{3+}(\text{DTTA})]$ and $[\text{Tb}^{3+}$

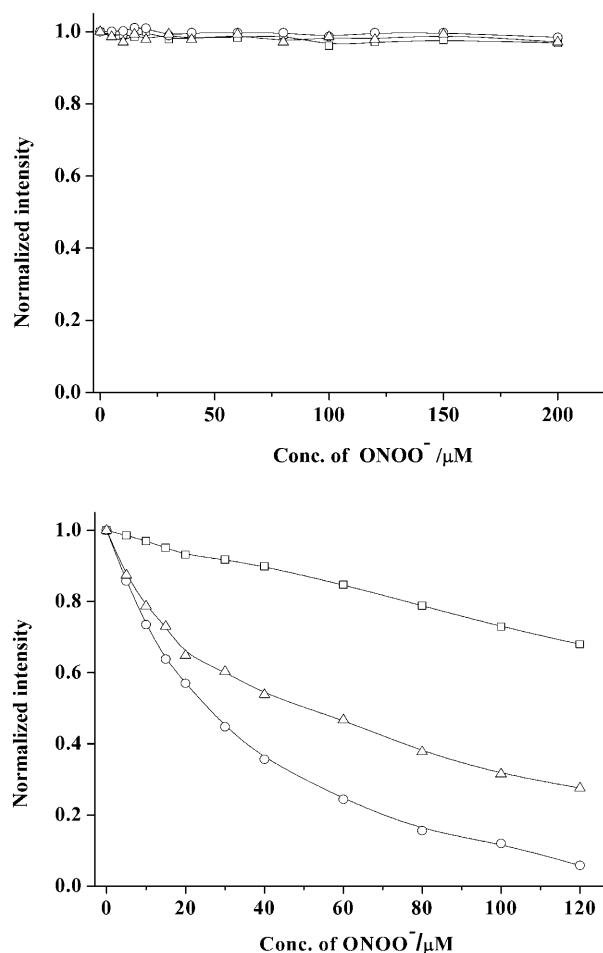


Figure 3. Optical responses (square: luminescence intensity; triangle: luminescence lifetime; circle: time-gated luminescence intensity) of [Eu³⁺(DTTA)] (2.0 μM) (top) and [Tb³⁺(DTTA)] (2.0 μM) (bottom) reacted with different concentrations of ONOO⁻.

(DTTA)] to different concentrations of ONOO⁻. Upon addition of different concentrations of ONOO⁻, [Eu³⁺(DTTA)] showed no change in optical properties (Figure 3, top); however, the luminescence intensity of [Tb³⁺(DTTA)] was decreased gradually. Moreover, the luminescence lifetime and time-gated luminescence intensity of [Tb³⁺(DTTA)] dramatically decreased (fitted to double exponential decays) with the increase of ONOO⁻ concentration. The results of luminescence titration experiments with ONOO⁻ also indicate that the time-gated excitation and emission spectra of [Eu³⁺(DTTA)] are almost unchanged (Figure 4, top) with the change of ONOO⁻ concentration, but those of [Tb³⁺(DTTA)] (Figure 4, bottom) are significantly changed. Unexpectedly, the LC/MS confirmation of the reaction product of [Tb³⁺(DTTA)] with ONOO⁻ showed that no nitrated product of [Tb³⁺(DTTA)] was formed. So the luminescence quenching of [Tb³⁺(DTTA)] by ONOO⁻ was not based on the d-PET mechanism. Early work has demonstrated that the lanthanide excited state can be deactivated by some electron-rich species, and the quenching of Tb³⁺ emission is greater than that of Eu³⁺ emission because the

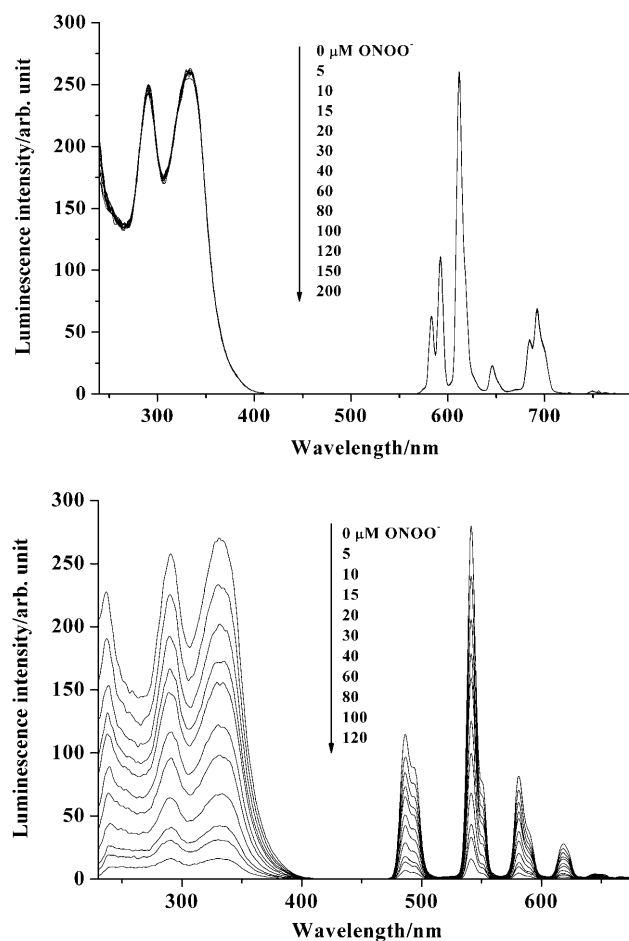


Figure 4. Time-gated excitation and emission spectra of [Eu³⁺(DTTA)] (2.0 μM) (top) and [Tb³⁺(DTTA)] (2.0 μM) (bottom) in the presence of different concentrations of ONOO⁻.

excited state energy level of the ⁵D₄ for Tb³⁺ (20400 cm⁻¹) is higher than that of the ⁵D₀ for Eu³⁺ (17200 cm⁻¹).^[11a,17] Thus, the quenching of the [Tb³⁺(DTTA)] luminescence by ONOO⁻ can be considered to occur by a charge-transfer mechanism, which has been examined more recently and shown to involve interaction of the electron-rich quenching species with the excited chromophore (exciplex).^[11d]

The different quenching behaviors of [Eu³⁺(DTTA)] and [Tb³⁺(DTTA)] observed above suggest that a mixture of [Eu³⁺(DTTA)] and [Tb³⁺(DTTA)] could be used as a ratiometric luminescence probe for ONOO⁻. Compared with luminescence-intensity-based probes, ratiometric luminescence probes allow the emission intensities at two different wavelengths to be measured; this process provides a built-in correction for environmental effects and increases the selectivity and sensitivity of the measurement. Accordingly, by using a “cocktail” of [Eu³⁺/Tb³⁺(DTTA)], the emission intensity ratio of the Eu³⁺/Tb³⁺ should be a direct function of the ONOO⁻ concentration. Figure 5 shows the time-gated emission spectra of [Eu³⁺/Tb³⁺(DTTA)] mixture in the presence of different concentrations of ONOO⁻. As expected, the luminescence intensity of Tb³⁺ emission was remarkably de-

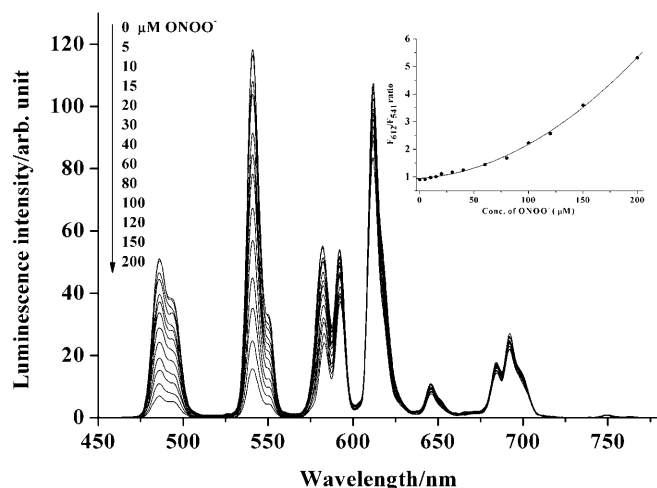


Figure 5. Time-gated emission spectra of $[\text{Eu}^{3+}/\text{Tb}^{3+}(\text{DTTA})]$ mixture (total concentration of $2.0 \mu\text{M}$, $\text{Eu}^{3+}/\text{Tb}^{3+}=1:2$) in the presence of different concentrations of ONOO^- (the inset shows the intensity ratio of F_{612}/F_{541} as a function of ONOO^- concentration).

creased upon addition of ONOO^- , but the response for Eu^{3+} emission was weak. The inset in Figure 5 shows the variation of the emission intensity ratio of Eu^{3+} (612 nm) to Tb^{3+} (541 nm) as a function of ONOO^- concentration. The curve, fitted to a double exponential correlation with a detection limit of $\approx 7 \mu\text{M}$, is similar to that of the reported lanthanide-complex-based ratiometric probe for uric acid.^[11a]

The specificity of luminescence response of the complex towards ONOO^- was also investigated. As shown in Figure 6 (top), the luminescence intensity changes of $[\text{Tb}^{3+}(\text{DTTA})]$ in the presence of ClO^- , $^1\text{O}_2$, O_2^- , H_2O_2 and NO_3^- are very small ($<5\%$) compared with the remarkable decrease (98%) in the presence of ONOO^- . It is notable that NO , $\cdot\text{OH}$ and NO_2^- also induced ≈ 20 , ≈ 30 , and $\approx 50\%$ decrease, respectively, in the luminescence intensity of $[\text{Tb}^{3+}(\text{DTTA})]$. It seems likely that NO , NO_2^- and other decomposition products of ONOO^- are also quenching species for the luminescence of $[\text{Tb}^{3+}(\text{DTTA})]$. However, when the $[\text{Eu}^{3+}/\text{Tb}^{3+}(\text{DTTA})]$ mixture was used as a ratiometric probe, the high specificity towards ONOO^- was obtained. As shown in Figure 6 (bottom), a 5.6-fold increase in F_{612}/F_{541} ratio can be observed when $[\text{Eu}^{3+}/\text{Tb}^{3+}(\text{DTTA})]$ is reacted with ONOO^- , whereas the reactions of $[\text{Eu}^{3+}/\text{Tb}^{3+}(\text{DTTA})]$ with NO , $^1\text{O}_2$, O_2^- , $\cdot\text{OH}$, ClO^- , H_2O_2 , and NO_3^- can not induce the change of F_{612}/F_{541} ratio (the change <0.1). Although a ≈ 0.7 -fold increase is observed in the presence of NO_2^- , this response is much weaker than that in the presence of ONOO^- . The specificity increase of the ratiometric probe is considered to be attributed to the overlapping of the Tb^{3+} emission at 617 nm and the Eu^{3+} emission at 612 nm, which causes the F_{612}/F_{541} ratio of the ratiometric probe to be also related to the F_{617}/F_{541} ratio of the Tb^{3+} luminescence. It is quite evident that the Tb^{3+} emission at 617 nm is beneficial to the specificity increase of the ratiometric probe.

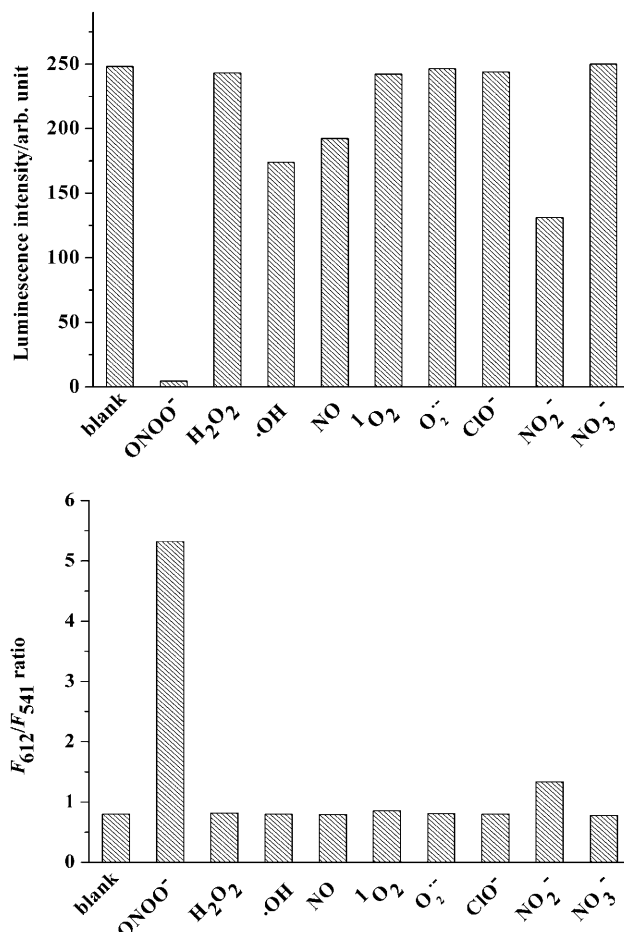


Figure 6. Time-gated luminescence intensity of $[\text{Tb}^{3+}(\text{DTTA})]$ ($2.0 \mu\text{M}$) (top) at 541 nm and F_{612}/F_{541} ratio of $[\text{Eu}^{3+}/\text{Tb}^{3+}(\text{DTTA})]$ mixture (total concentration of $2.0 \mu\text{M}$, $\text{Eu}^{3+}/\text{Tb}^{3+}=1:2$) (bottom) in the presence of various ROS ($200 \mu\text{M}$) at room temperature.

The luminescence quenching kinetics of ONOO^- - $[\text{Tb}^{3+}(\text{DTTA})]$ system was determined by real-time recording the time-gated luminescence intensity change of $[\text{Tb}^{3+}(\text{DTTA})]$ after addition of ONOO^- . As shown in Figure 7, upon addition of different concentrations of ONOO^- , the luminescence intensity of $[\text{Tb}^{3+}(\text{DTTA})]$ decreased rapidly, and achieved a steady value in a very short time ($<3 \text{ s}$). This result indicates that the luminescence quenching of the ONOO^- - $[\text{Tb}^{3+}(\text{DTTA})]$ system is very fast, which is favorable for the detection of short-lived ONOO^- in neutral aqueous solutions ($t_{50} < 1 \text{ s}$).^[18]

Luminescence imaging of ONOO^- in living cells: The cultured HeLa cells were used to investigate the potential of the new probe for the luminescence imaging detection of ONOO^- in living systems. When the cells were co-incubated with $[\text{Tb}^{3+}(\text{DTTA})]$, no luminescent cells were observed in the time-gated mode, indicating that $[\text{Tb}^{3+}(\text{DTTA})]$ cannot permeate through the cell membrane into the cells. After co-incubating with AM-DTTA and Tb^{3+} ions, bright cyan (mixture of blue and green from cell components and the

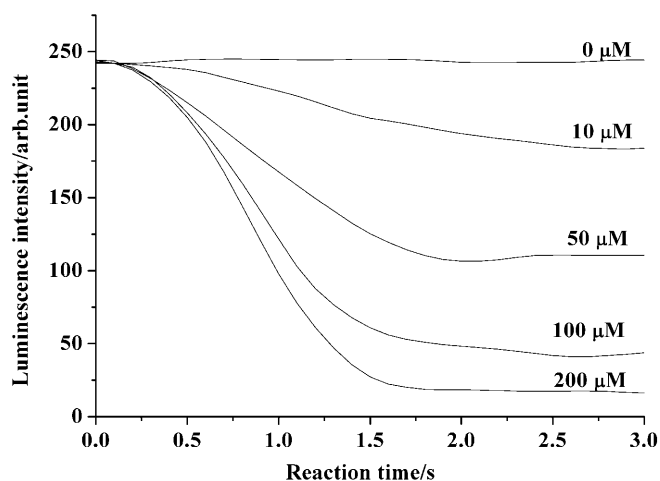


Figure 7. Luminescence quenching kinetic curves of $[\text{Tb}^{3+}(\text{DTTA})]$ ($2.0 \mu\text{M}$) at different concentrations of ONOO^- in 0.05 M Tris-HCl buffer of pH 7.4.

Tb^{3+} complex) luminescence and a strong green time-gated luminescence (from the Tb^{3+} complex) from the cells were observed (Figure 8A). When the $[\text{Tb}^{3+}(\text{DTTA})]$ -loaded HeLa cells were treated with a ONOO^- donor, 3-morpholinonydnonimine (SIN-1), for 30 min, both normal luminescence and time-gated luminescence intensities of the cells gradually decreased with increasing SIN-1 concentration (Figure 8B and 8C). The above results demonstrate that AM-DTTA and Tb^{3+} ions can be easily transferred into the cultured HeLa cells by an ordinary incubation method. After hydrolysis of the acetoxymethyl ester by ubiquitous

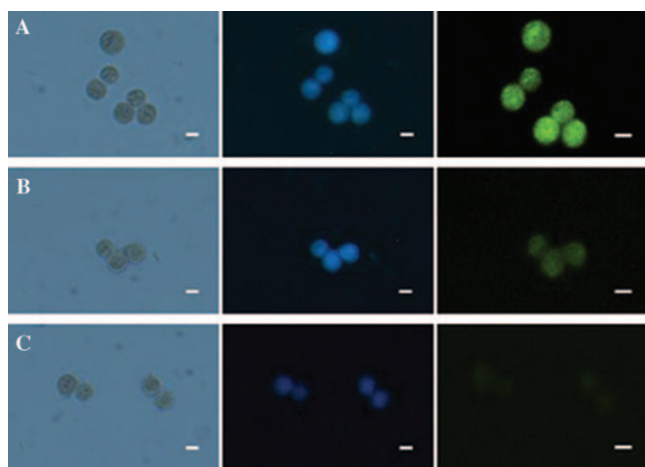


Figure 8. Bright-field (left), normal luminescence (middle), and time-gated luminescence (right) images of the $[\text{Tb}^{3+}(\text{DTTA})]$ -loaded HeLa cells in the presence of ONOO^- . The $[\text{Tb}^{3+}(\text{DTTA})]$ -loaded cells were prepared by incubating HeLa cells in the culture medium (1.0 mL) containing a freshly prepared solution of AM-DTTA (0.5 mM of total DTTA) and Tb^{3+} (0.5 mM) for 2 h at 37°C in a $5\% \text{ CO}_2/95\% \text{ air}$ incubator, and were further incubated in the isotonic saline solution containing different concentrations of SIN-1 (A: negative control; B: $500 \mu\text{M}$ of SIN-1; C: 1.0 mM of SIN-1) for another 30 min, and then used for the luminescence microscopy imaging detection. Scale bars: $10 \mu\text{m}$. The time-gated luminescence images are shown in pseudo-color (wavelength of 545 nm) treated by a SimplePCI software.^[9a]

intracellular esterases, the stable and cell-membrane-impermeable $[\text{Tb}^{3+}(\text{DTTA})]$ molecules are regenerated and loaded within the cells, which enables $[\text{Tb}^{3+}(\text{DTTA})]$ to be used as a probe for the time-gated luminescence imaging detection of ONOO^- in living cells.

The $[\text{Eu}^{3+}/\text{Tb}^{3+}(\text{DTTA})]$ -loaded HeLa cells were also prepared by co-incubating the cells with AM-DTTA and $\text{Eu}^{3+}/\text{Tb}^{3+}$ ($\text{Eu}^{3+}/\text{Tb}^{3+} = 1:2$) mixture. In this case, the strong hybrid luminescence (pale blue) from the cells was observed (Figure 9A). After treatment with different concentrations of SIN-1 for 30 min, the color changes of the cells from pale pink to red were observed (Figure 9B to 9D). This phenomenon can be explained as follows. Upon addition of SIN-1, the luminescence of $[\text{Tb}^{3+}(\text{DTTA})]$ was gradually quenched, while that of $[\text{Eu}^{3+}(\text{DTTA})]$ was not, which caused the increase of the emission intensity ratio of the $\text{Eu}^{3+}/\text{Tb}^{3+}$ in the cells, yielding a series of luminescence

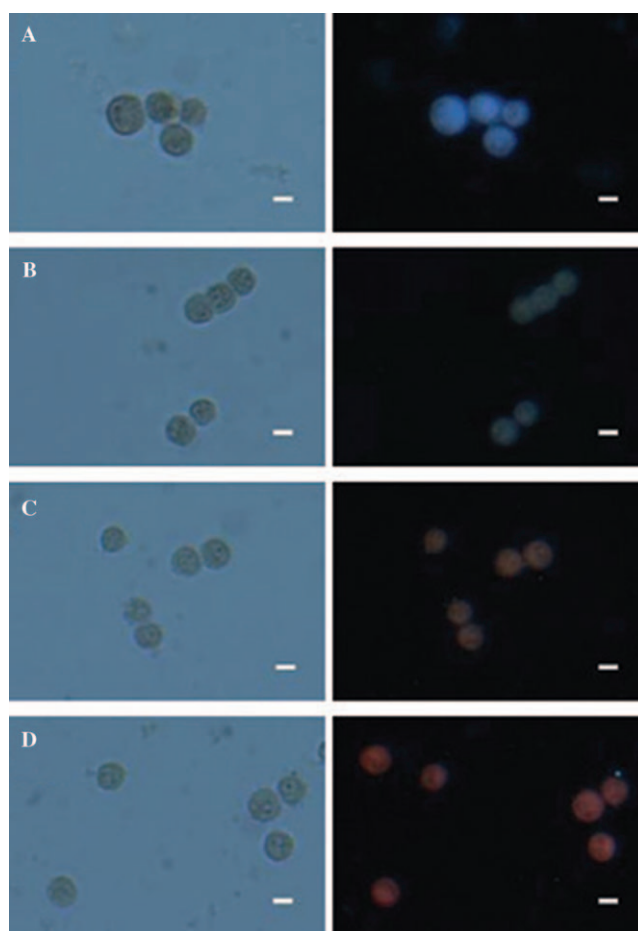


Figure 9. Bright-field (left) and normal luminescence (right) images of the $[\text{Eu}^{3+}/\text{Tb}^{3+}(\text{DTTA})]$ -loaded HeLa cells in the presence of ONOO^- . The $[\text{Eu}^{3+}/\text{Tb}^{3+}(\text{DTTA})]$ -loaded cells were prepared by incubating HeLa cells in the culture medium (1.0 mL) containing a freshly prepared solution of AM-DTTA (0.5 mM of total DTTA) and $\text{Eu}^{3+}/\text{Tb}^{3+}$ mixture (0.5 mM , $\text{Eu}^{3+}/\text{Tb}^{3+} = 1:2$) for 2 h at 37°C in a $5\% \text{ CO}_2/95\% \text{ air}$ incubator, and were further incubated in the isotonic saline solution containing different concentrations of SIN-1 (A: negative control; B: $100 \mu\text{M}$ of SIN-1; C: $200 \mu\text{M}$ of SIN-1; D: $500 \mu\text{M}$ of SIN-1) for another 30 min, and then used for the luminescence microscopy imaging detection. Scale bars: $10 \mu\text{m}$.

color changes of the cells. Since the luminescence color change is easier observed than the luminescence intensity change, the ratiometric luminescence probe $[\text{Eu}^{3+}/\text{Tb}^{3+}(\text{DTTA})]$ is more favorable to be used for the sensitive and selective detection of ONOO^- in living cells compared with other intensity-based luminescent probes. Due to the lack of a true-color time-gated luminescence microscope, the performance of this ratiometric luminescence probe for imaging ONOO^- with time-gated mode to eliminate the effect of autofluorescence from the cells was not determined.

To examine the intracellular retention of the probe, $[\text{Eu}^{3+}(\text{DTTA})]$ -loaded HeLa cells were prepared. After washing twice with the isotonic saline solution, luminescence images of the cells were determined over a period of 30 min at 10 min intervals (Figure 10). As expected, there were no

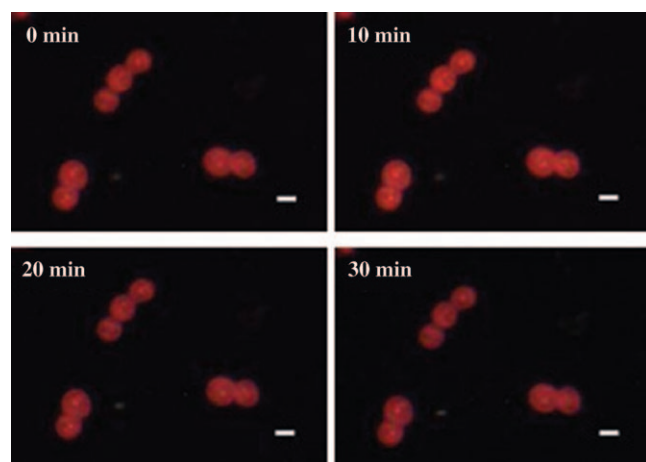


Figure 10. Luminescence images of the $[\text{Eu}^{3+}(\text{DTTA})]$ -loaded HeLa cells in the isotonic saline solution within 30 min. The $[\text{Eu}^{3+}(\text{DTTA})]$ -loaded cells were prepared by incubating HeLa cells in the culture medium (1.0 mL) containing freshly prepared solution of AM-DTTA (0.5 mM of total DTTA) and Eu^{3+} (0.5 mM) for 2 h at 37 °C in a 5% $\text{CO}_2/95\%$ air incubator. Scale bars, 10 μm .

changes of the luminescence images in the period of 30 min, indicating that the probe $[\text{Eu}^{3+}(\text{DTTA})]$ in the cells could not be transferred to the outside solution. This result demonstrates that, compared with conventional organic fluorescent probes, the new $[\text{Ln}^{3+}(\text{DTTA})]$ probe has superior intracellular retention and is more favorable to be used for the visualization and continuous observation of ONOO^- in living systems. In addition, the result of a trypan blue experiment shows that the $[\text{Ln}^{3+}(\text{DTTA})]$ -loaded HeLa cells still retain their activity, which indicates that the effect of the probe on the viability of the cells is low.

Conclusion

By incorporating a 2,4-dimethoxyphenyl moiety into a lanthanide luminophore, $(2,2':6',2''\text{-terpyridine-6,6''-diyl})\text{-bis}(\text{methylenenitrilo})\text{tetrakis}(\text{acetate})\text{-Eu}^{3+}/\text{Tb}^{3+}$, $[\text{Eu}^{3+}/\text{Tb}^{3+}(\text{DTTA})]$, the first lanthanide-complex-based ratiomet-

ric luminescence probe specific for ONOO^- was successfully developed. This probe can specifically and rapidly recognize ONOO^- , resulting from remarkable luminescence quenching for $[\text{Tb}^{3+}(\text{DTTA})]$, but no response for $[\text{Eu}^{3+}(\text{DTTA})]$. Compared with previously reported ONOO^- luminescence probes, the new probe has the advantages of good specificity, sensitivity, kinetic and thermodynamic stabilities, water solubility, wide pH available range, and the applicability for ratiometric and time-gated measurements. The results of luminescence imaging by monitoring ONOO^- in living cells demonstrated the utility of the probe for in vivo ONOO^- detection. The new luminescence probe, with fine ratiometric and time-gated capacities, provides a novel strategy for visualizing the temporal and spatial distribution of ONOO^- in cells and biological tissues, which would be a useful tool for investigating the pathogenic role of ONOO^- in biological systems.

Experimental Section

Materials: The ONOO^- solution was prepared according to the literature method,^[19] and was stored at $-30\text{ }^\circ\text{C}$. The concentration was determined by using its molar extinction coefficient of $1670\text{ M}^{-1}\text{ cm}^{-1}$ at 302 nm before use.^[7a] 1-Hydroxy-2-oxo-3-(3-aminopropyl)-3-methyl-1-triazene (NOC-13) was synthesized by using a reported method.^[20] Bromomethyl acetate and 3-morpholinopyridone (SIN-1) were purchased from Sigma-Aldrich. HeLa cells were obtained from Dalian Medical University. The isotonic saline solution consisting of 140 mM NaCl, 10 mM glucose, and 3.5 mM KCl was prepared in our laboratory. Deionized and distilled water was used throughout. Unless otherwise stated, all chemical materials were purchased from commercial sources and used without further purification.

Physical measurements: The ^1H NMR spectra were measured on a Bruker DRX 400 spectrometer (400 MHz). The MS spectra were recorded on a HP1100 LC/MSD electrospray ionization mass spectrometry (ESI/MS). Elemental analysis was carried out on a Vanio-EL CHN analyzer. Melting points were determined on a WRS-1B digital melting-point apparatus. Absorption spectra were measured on a Perkin-Elmer Lambda 35 UV/Vis spectrometer. Time-gated luminescence spectra were measured on a Perkin-Elmer LS 50B spectrofluorometer with the settings of delay time, 0.2 ms; gate time, 0.4 ms; cycle time, 20 ms; excitation slit, 10 nm; and emission slit, 5 nm. Luminescence quantum yields were measured by using the previously reported methods.^[10] HPLC analysis was carried out on a SinoChrom ODS-BP 5 μm ($4.6\times 250\text{ mm}$) column by using an HPLC system consisting of two pumps (Elite P230) and a detector (Elite UV 230+). All normal luminescence imaging and time-gated luminescence imaging measurements were carried out on a laboratory-use luminescence microscope.^[9a] The microscope (TE2000-E; Nikon), equipped with a 100 W mercury lamp, a UV-2A filters (Nikon, excitation filter, 330–380 nm; dichroic mirror, 400 nm; emission filter, $>420\text{ nm}$) and a color CCD camera system (RET-2000R-F-CLR-12-C, Qimaging) was used for the normal luminescence imaging measurement with an exposure time of 20 s. The microscope, equipped with a 30 W xenon flash-lamp (Pulse300, Photonic Research Systems), UV-2A filters and a time-gated digital black-and-white CCD camera system (Photonic Research Systems) was used for the time-gated luminescence measurement with the conditions of delay time, 50 μs ; gate time, 1000 μs ; lamp pulse width, 6 μs ; and exposure time, 90 s.

Synthesis of the ligand DTTA: The details of the DTTA synthesis are shown in Supporting Information.

Synthesis of the acetoxymethyl ester of DTTA (AM-DTTA): A solution of DTTA (18.5 mg, 0.025 mmol), dry triethylamine (14.6 mg, 1.30 mmol), and bromomethyl acetate (37.5 mg, 0.25 mmol) in dry dimethyl sulfoxide

(0.5 mL) was stirred at room temperature overnight. The resulting brown mixture containing AM-DTTA and un-esterified DTTA was used for the cell imaging experiment without further purification. ESI-MS (m/z) for AM-DTTA: m/z (%): 948.3 (25) $[M+H]^+$.

Reactions of $[Ln^{3+}(DTTA)]$ with ROS: All the reactions were carried out in the air-saturated 0.05 M Tris-HCl buffer of pH 7.4 with the same concentration of $[Tb^{3+}(DTTA)]$ (2.0 μ M) or $[Eu^{3+}/Tb^{3+}(DTTA)]$ (total concentration of 2.0 μ M, $Eu^{3+}/Tb^{3+}=1:2$) for 30 min at room temperature. Various ROS were generated with the following procedures. Hydrogen peroxide and hypochlorite were delivered from 30 and 10% aqueous solutions, respectively. Prior to use, hydrogen peroxide was assayed by using its molar absorption coefficient of $43.6\text{ M}^{-1}\text{ cm}^{-1}$ at 240 nm.^[21] Superoxide solution ($O_2^{\cdot-}$) was prepared by dissolving solid KO_2 in dry dimethyl sulfoxide and the mixture was stirred vigorously for 10 min before use. Hydroxyl radical ($\cdot OH$) was generated by the Fenton reaction between ferrous ammonium sulfate and hydrogen peroxide.^[9a] NO was generated by using NOC-13 as an NO donor.^[20] Singlet oxygen (1O_2) was generated by the reaction of hypochlorite with hydrogen peroxide.^[22] The stock solution of ONOO⁻ was used throughout.

Detection of reaction kinetics of $[Tb^{3+}(DTTA)]$ with ONOO⁻: The reaction kinetics between $[Tb^{3+}(DTTA)]$ and ONOO⁻ was determined in the air-saturated 0.05 M Tris-HCl buffer of pH 7.4 at room temperature. After the ONOO⁻ solution was added to $[Tb^{3+}(DTTA)]$ solution (2.0 μ M), the kinetic curve was recorded immediately on a Perkin-Elmer LS 50B luminescence spectrometer with a time-gated luminescence mode with the settings of delay time, 0.2 ms; gate time, 0.4 ms; cycle time, 20 ms; excitation wavelength, 335 nm; emission wavelength, 541 nm; excitation slit, 10 nm; emission slit, 5 nm; and data interval, 0.1 s.

Detection of ONOO⁻ in aqueous media: The reactions of $[Eu^{3+}(DTTA)]$, $[Tb^{3+}(DTTA)]$, and $[Eu^{3+}/Tb^{3+}(DTTA)]$ with ONOO⁻ were carried out in the air-saturated 0.05 M Tris-HCl buffer of pH 7.4 at room temperature. A series of ONOO⁻ solutions at different concentrations were added to the buffer solutions containing 2 μ M of $[Eu^{3+}(DTTA)]$, $[Tb^{3+}(DTTA)]$, or $[Eu^{3+}/Tb^{3+}(DTTA)]$ ($Eu^{3+}/Tb^{3+}=1:2$). After stirring for 15 min, the time-gated excitation and emission spectra were measured.

Luminescent cell imaging: HeLa cells were cultured in RPMI-1640 medium, supplemented with 10% fetal bovine serum, 1% penicillin, and 1% streptomycin at 37°C in a 5% $CO_2/95\%$ air incubator. For ONOO⁻ imaging detection, the $[Tb^{3+}(DTTA)]$ - or $[Eu^{3+}/Tb^{3+}(DTTA)]$ -loaded cells were prepared by adding AM-DTTA and Tb^{3+} or AM-DTTA and Eu^{3+}/Tb^{3+} into the culture medium of HeLa cells (4×10^5 cells mL^{-1}) according to the conditions as described in the legend of Figures 8–10. After incubation for 2 h at room temperature, the cells were separated by centrifugation at 1000 rpm, washed three times with the isotonic saline solution, and confirmed with the trypan blue experiment. The cells were further incubated in the isotonic saline solution containing the ONOO⁻ donor SIN-1 for another 30 min, and then spotted on a glass slide for luminescence microscopy imaging detection.

Acknowledgements

Financial supports from the National Natural Science Foundation of China (Nos. 20835001, 20975017) and the Specialized Research Fund for the Doctoral Program of Higher Education of China (No. 200801410003) are gratefully acknowledged.

- [1] a) G. Ferrer-Sueta, R. Radi, *ACS Chem. Biol.* **2009**, *4*, 161–177; b) C. Szabó, H. Ischiropoulos, R. Radi, *Nat. Rev. Drug Discov.* **2007**, *6*, 662–680; c) B. Alvarez, R. Radi, *Amino Acids* **2003**, *25*, 295–311; d) P. Pacher, J. S. Beckman, L. Liaudet, *Physiol. Rev.* **2007**, *87*, 315–424.

- [2] a) H. Wiseman, B. Halliwell, *Biochem. J.* **1996**, *313*, 17–29; b) P. Liu, B. H. Xu, J. Quilley, P. Y. K. Wong, *Am. J. Physiol.* **2000**, *279*, 1970–1977; c) A. Midori, M. D. Yenari, *Cleveland Clin. J. Med.* **2004**, *71*, S25–S27; d) C. R. White, T. A. Brock, L. Chang, J. Crapo, P. Briscoe, D. Ku, W. A. Bradley, S. H. Gianturco, J. Gore, B. A. Freeman, M. M. Tarpey, *Proc. Natl. Acad. Sci. USA* **1994**, *91*, 1044–1048; e) J. S. Beckman, M. Carson, C. D. Smith, W. H. Koppenol, *Nature* **1993**, *364*, 584–585.
- [3] a) A. Vandervliet, J. P. Eiserich, C. A. O'Neill, B. Halliwell, C. E. Cross, *Arch. Biochem. Biophys.* **1995**, *319*, 341–349; b) K. Dai, A. G. Vlessidis, N. P. Evmiridis, *Talanta* **2003**, *59*, 55–65; c) S. B. Digerness, K. D. Harris, J. W. Kirklin, *Free Radical Biol. Med.* **1999**, *27*, 1386–1392; d) J. Xue, X. Ying, J. Chin, *Anal. Chem.* **2000**, *72*, 5313–5321; e) S. Dikalov, M. Skatchkov, E. Basseneg, *Biochem. Biophys. Res. Commun.* **1997**, *230*, 54–57.
- [4] J. P. Y. Kao, *Methods Cell Biol.* **1994**, *40*, 155–181.
- [5] a) H. Possel, H. Noack, W. Augustin, G. Keilhoff, G. Wolf, *FEBS Lett.* **1997**, *416*, 175–178; b) N. W. Kooy, J. A. Royall, H. Ischiropoulos, J. S. Beckman, *Free Radical Biol. Med.* **1994**, *16*, 149–156.
- [6] T. Ueno, Y. Urano, H. Kojima, T. Nagano, *J. Am. Chem. Soc.* **2006**, *128*, 10640–10641.
- [7] a) D. Yang, H. Wang, Z. Sun, N. Chung, J. Shen, *J. Am. Chem. Soc.* **2006**, *128*, 6004–6005; b) Z. Sun, H. Wang, F. Liu, Y. Chen, P. K. H. Tam, D. Yang, *Org. Lett.* **2009**, *11*, 1887–1890.
- [8] a) H. Li, H. Yan, *J. Phys. Chem. C* **2009**, *113*, 7526–7530; b) W. Lin, L. Long, B. Chen, W. Tan, *Chem. Eur. J.* **2009**, *15*, 2305–2309.
- [9] a) B. Song, G. L. Wang, M. Q. Tan, J. L. Yuan, *J. Am. Chem. Soc.* **2006**, *128*, 13442–13450; b) K. Hanaoka, K. Kikuchi, S. Kobayashi, T. Nagano, *J. Am. Chem. Soc.* **2007**, *129*, 13502–13509; c) K. Ai, B. Zhang, L. Lu, *Angew. Chem.* **2009**, *121*, 310–314; *Angew. Chem. Int. Ed.* **2009**, *48*, 304–308.
- [10] a) B. Song, G. L. Wang, J. L. Yuan, *Chem. Commun.* **2005**, 3553–3555; b) M. Q. Tan, B. Song, G. L. Wang, J. L. Yuan, *Free Radical Biol. Med.* **2006**, *40*, 1644–1653.
- [11] a) R. Poole, F. Kielar, S. L. Richardson, P. A. Stenson, D. Parker, *Chem. Commun.* **2006**, 4084–4086; b) M. S. Tremblay, M. Halim, D. Sames, *J. Am. Chem. Soc.* **2007**, *129*, 7570–7577; c) G. L. Law, R. Pal, L. O. Palsson, D. Parker, K. L. Wong, *Chem. Commun.* **2009**, 7321–7323; d) G. L. Law, D. Parker, S. L. Richardson, K. L. Wong, *Dalton Trans.* **2009**, 8481–8484.
- [12] a) R. Y. Tsien, *Nature* **1981**, *290*, 527–528; b) R. P. Haugland in *The Handbook: A Guide to Fluorescent Probes and Labeling Technologies*, 10th ed. (Ed.: M. T. Z. Spence), Invitrogen Corporation, Karlsruhe, **2005**, pp. 881–885.
- [13] a) I. Hemmilä, V. M. Mikkala, *Crit. Rev. Clin. Lab. Sci.* **2001**, *38*, 441–519; b) J. L. Yuan, G. L. Wang, *TrAC Trends Anal. Chem.* **2006**, *25*, 490–500; c) S. V. Eliseeva, J. C. G. Bünzli, *Chem. Soc. Rev.* **2010**, *39*, 189–227.
- [14] M. Latva, H. Takalo, V. M. Mikkala, C. Matachescu, J. C. Rodríguez-Ubis, J. Kankare, *J. Lumin.* **1997**, *75*, 149–169.
- [15] M. H. V. Werts, J. W. Verhoeven, J. W. Hofstraat, *J. Chem. Soc. Perkin Trans. 2* **2000**, 433–439.
- [16] A. Beeby, I. M. Clarkson, R. S. Dickens, S. Faulkner, D. Parker, L. Royle, A. S. De Sousa, J. A. G. Williams, M. Woods, *J. Chem. Soc. Perkin Trans. 2* **1999**, 493–504.
- [17] R. A. Poole, G. Bobba, M. J. Cann, J. C. Frias, D. Parker, R. D. Peacock, *Org. Biomol. Chem.* **2005**, *3*, 1013–1024.
- [18] N. Ashki, K. C. Hayes, F. Bao, *Neuroscience* **2008**, *156*, 107–117.
- [19] J. W. Reed, H. H. Ho, W. L. Jolly, *J. Am. Chem. Soc.* **1974**, *96*, 1248–1249.
- [20] J. A. Hrabie, J. R. Kclose, *J. Org. Chem.* **1993**, *58*, 1472–1476.
- [21] B. Lei, N. Adachi, T. Arai, *Brain Res. Protoc.* **1998**, *3*, 33–36.
- [22] A. M. Held, D. J. Halko, J. K. Hurst, *J. Am. Chem. Soc.* **1978**, *100*, 5732–5740.

Received: March 1, 2010
Published online: May 19, 2010